

# Nanowire Bolometers

J. B. Peterson<sup>a</sup>, A. T. Bollinger<sup>b</sup>, A. Berzyadin<sup>b</sup>, D. Bock<sup>a</sup> and K. Garcia<sup>ac</sup>

<sup>a</sup>Dept. of Physics, Carnegie Mellon University, Pittsburgh, PA 15217

<sup>b</sup>Dept. of Physics, University of Illinois Urbana - Champaign, Urbana, IL, 61801

<sup>c</sup>Dept. of Physics and Astronomy, Rice University, Houston TX, 77005

## ABSTRACT

Cryogenic tests of a prototype superconducting nanowire bolometer are presented. The device has such low thermal conductance it should be sensitive when used as a direct detector. Because of the small size of the active area we anticipate that this bolometer may also be fast enough to be used as a wideband mixer.

**Keywords:** bolometer, detector, nanowire, nanotube, superconductor, hot electron bolometer, mixer, sub-millimeter, millimeter-wave

## 1. INTRODUCTION

In the wavelength range 100 microns to 3 mm bolometers<sup>1</sup> are among the most sensitive detectors available for broadband astronomical observations. Examples of recent uses of bolometers include: at millimeter wavelengths—photometry and polarimetry of the Cosmic Microwave Background and the study dust enshrouded galactic nuclei; at sub-millimeter wavelengths—searches for thermal emission from dusty protogalaxies and polarimetric mapping of magnetic fields in the dense region near the Galactic center. As bolometer sensitivity improves these detectors will be useful in narrower bandwidth applications such as searches for the emission and absorption lines of high redshift galaxies.

Any detector of electromagnetic radiation can also be used as a mixer. If a detector is fast enough to respond to the beat frequency between two signals applied simultaneously, the down conversion product (IF) of an applied pair (RF and LO) of input signals will be present at the detector output. Bolometers respond *thermally* to the radiation they are being used to detect.<sup>2,3</sup> So, for a bolometer used as a mixer, the bandwidth is  $B \sim 1/\tau$  where  $\tau$  is the thermal time constant.<sup>4</sup> It might seem that bolometers would be slower than other detectors and therefore of limited application as mixers, but some antenna coupled bolometers have been found to respond with  $\sim 100ps$  time constant and offer bandwidth approaching 10 GHz.<sup>3</sup>

A bolometer employs a thermally isolated absorber for electromagnetic radiation: this converts incoming radiation to heat. The absorber is connected to a cold reservoir (the “bath”) by a link with low thermal conductance. The temperature rise resulting from arriving radiation is sensed by a thermometer. This temperature sensor can be electrically isolated from the absorber—this is called a composite bolometer—or the absorber itself can have DC resistance that depends on temperature.<sup>5</sup>

When using a bolometer as a detector isolating the bolometer thermally (reducing the thermal conductance  $G$ ) will make the detector responsive to arriving radiation. However increasing thermal isolation can increase the thermal response<sup>6</sup> time  $\tau = C/G$  ( $C$  is the heat capacity) and limit the mixing bandwidth. So, in previous designs, it has been necessary to optimize the design<sup>7</sup> either for detection or for mixing.<sup>8</sup>

The primary goal of astronomical bolometer design is to achieve sensitivity limited by the fluctuations of the arriving photons from the cold sky. This requires that the bolometer itself be colder than the sky.<sup>9</sup> As an example, a bolometer used to study the 3K Cosmic Microwave Background will generally operate at a temperatures below 0.3K.

At sub-kelvin temperatures the electron system in a metallic solid generally has only weak thermal contact with the lattice the electrons occupy. Then incoming radiation, dissipated by the electron system, can raise

---

Further author information: JBP: E-mail: jbp@cmu.edu, AB: E-mail: bezryadi@uiuc.edu



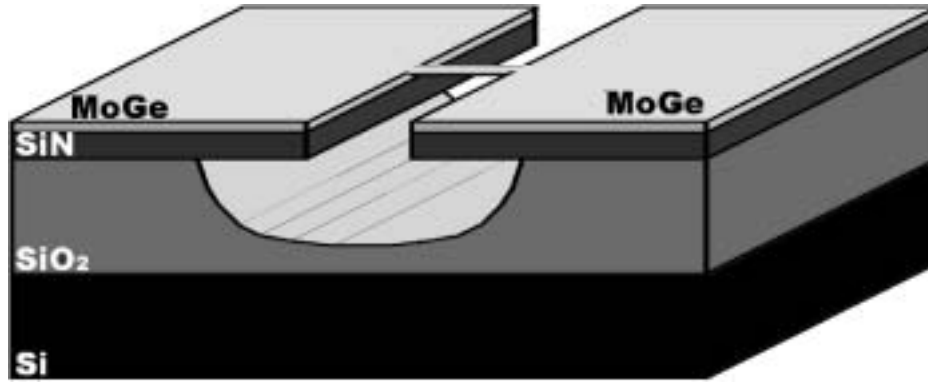


**Figure 1.**

**Nanotube Substrate for Nanowire.** A fluorinated carbon nanotube placed across an undercut groove forms the substrate for deposition of the MoGe nanowire.

the electron temperature without significant increase in the temperature of the lattice. Such a device is called a hot-electron bolometer. Recently hot-electron bolometers have been developed that employ sub-micron size absorbing elements.<sup>2</sup> Because such an absorber is much smaller than the wavelength of the arriving radiation, the absorber must be coupled to the radiation stream by an antenna if high efficiency is to be achieved. The absorber is the termination load for the antenna. The combined system has radiation collection cross-section  $\sim \lambda^2$ . This is called an antenna coupled bolometer.

As the dimensions of the absorbing element are reduced the thermal conductance  $G$  is reduced, *and* the time constant is reduced. Using nanometer fabrication techniques it should be possible to create an antenna-coupled hot-electron bolometer with the low  $G$  needed to work as a sensitive detector, which also has the thermal response speed needed to work as a wideband mixer.

In this paper we report on cryogenic tests of a nanometer-size bolometer prototype, consisting of a superconducting nanowire. We find the thermal conductance  $G$  of the nanowire is in the range  $10^{-9}$  to  $10^{-11}$  W/K, which is just the range needed for broadband millimeter and sub-millimeter astronomy. Since the absorbing region of the bolometer contains only about 10 million atoms the heat capacity of the device must be very small and we expect the device to offer a wide bandwidth when used as a mixer. We have not yet connected a nanowire to an antenna.

## 2. FABRICATION

The nanowire we report on was fabricated<sup>10</sup> on a fluorinated carbon nanotube. The nanotube spans an undercut groove etched in a silicon nitride coating on a silicon substrate, as shown in Figure 1. A thin coating of Molybdenum-Germanium is then sputtered on the nanotube and the silicon nitride surfaces, creating the nanowire and thin film contact regions at each end.<sup>11</sup> A scanning electron micrograph of such a nanowire is shown in figure 2. The dimensions of the wire are approximately thickness—7 nm, width—15 nm, length—100 nm. Molybdenum-Germanium was chosen to create the wire because it forms uniform films even for very thin layers.

## 3. CRYOGENIC TESTS

The nanowire was fabricated primarily to study superconductivity in very thin wires. The superconducting transition temperature in bulk Molybdenum-Germanium is about 8K. The low-current resistance of the nanowire device is shown in the inset in figure 3. The device exhibits two increases in resistance as the temperature is increased, at 3.5 K and 6 K. We interpret these increases as the onset of dissipation in the wire and the contact



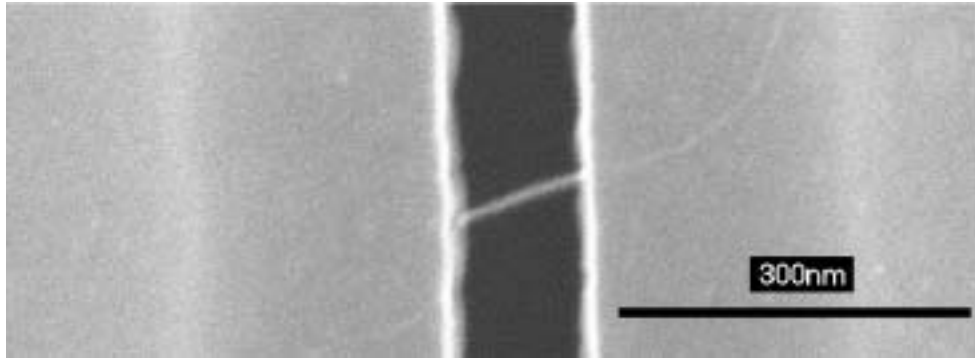


**Figure 2.**

**Electron Micrograph of Nanowire.** The dimensions of the nanowire are approximately: thickness-7; width-15; length-100 nanometers

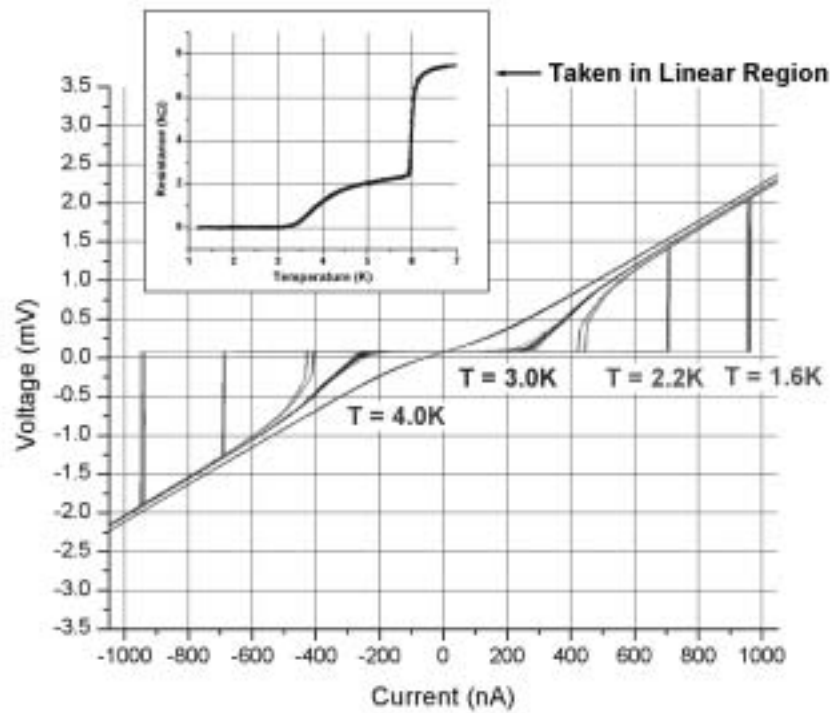


**Figure 3.**

**Electrical Response of Nanowire.** The inset shows the linear resistance of the wire for small currents. The two increases in resistance at 3.5 K and 6.0 K are attributed to transitions from superconducting to resistive state in the narrow wire (3.5 K) and the wider, thin film pad regions outside the narrow wire region. The transition temperature in bulk material is about 8K. The main panel shows the current versus voltage for four bath temperatures. For bath temperatures below the wire transition temperature the IV curve is strongly non-linear and hysteretic. The hysteresis curve for 2.2K bath temperature lies inside the curve for 1.6K. We interpret this non-linear behavior as the result of ohmic heating of the nanowire.



regions respectively. This suppression of  $T_c$  along with the broadening of the transition is expected<sup>12</sup> in thin wires and films.

For currents between 200 nA and 1000 nA, for bath temperatures below 3.5 K, the IV curves for the device are strongly non-linear and exhibit hysteresis. Regardless of the reason for this nonlinearity, its presence indicates that the device should be useful as a detector.

We interpret the IV curves as follows: Beginning at zero current the wire is superconducting, so as the current rises, the wire initially has no voltage across it. Eventually, the current exceeds the limiting value for zero dissipation, and a voltage develops across the wire. This dissipation raises the electron temperature in the wire which further increases the resistance. Decreasing the current from this point does not immediately restore the zero dissipation state in the wire since the electrical dissipation maintains a higher temperature in the wire than with the current rising. As the current falls, eventually, as the center of the wire approaches 3.5K, the resistance declines and dissipation is reduced. Further decrease of the current results in a sudden drop of the voltage as the wire returns to the zero dissipation state.

Note that for currents above 1000 nA the IV curve is linear, but the intercept of the line falls at a current above zero. This might be explained as a variation of resistance with current in the dissipative state. Such variation might occur if super-currents persist in the wire but dissipate energy via phase slips.

The IV curve of the wire resembles that of a superconductor-insulator-superconductor tunnel junction. It is possible that we are incorrectly interpreting the IV curves, and that the nonlinear curve is not due to thermal effects but instead to tunneling at one or both wire-contact junction. However, the strong hysteresis of the IV curve favors a thermal model.

Another reason to trust a thermal model to explain the IV curves in figure 3 is that the bulk thermal conductivity estimated from the conductance values we derive is in the range 0.06 to 2 W/Km. This falls close to typical thermal conductivity values for alloys at these temperatures.

Continuing with a thermal interpretation of the IV curves, we can estimate the thermal conductance of the nanowire. Even though the temperature peaks at the center of the wire we simplify the thermal model by assigning a single temperature to the wire. The effective conductance  $G = IV/\Delta T$  is then determined using the resistance  $R = V/I$ , and the  $R(T)$  relation plotted in the inset of figure 3. The resulting  $G$  values are plotted in figure 4. For each assumed wire temperature we get similar values of  $G$  for all bath temperatures. This internal consistency gives us some confidence that we are on track with our thermal model.

#### 4. THERMAL CONDUCTANCE

We find the wire thermal conductance increases dramatically with temperature. This seems reasonable since as the wire warms the fraction of charge carriers bound together as Cooper pairs decreases and the fraction of unpaired, thermally excited fermionic carriers increases. Unpaired electrons carry heat, Cooper pairs do not. Fitting the conductance to a thermally activated fermion model we find the carrier activation temperature is about 30 K, around four times higher than the expected value,  $T_{c,bulk}$ . We do not yet understand this discrepancy.

At the  $\sim 4$  K wire temperatures of these experiments the nanowire may not be operating in the hot-electron regime. Instead the electrons may be heating the lattice and phonons may be important as carriers of heat. In a hot-electron bolometer unpaired-electron diffusion is the dominant cooling mechanism and the thermal conductance is related to the electrical resistance according to the Wiedemann-Franz law.<sup>13</sup> For our nanowire the maximum thermal conductance calculated from the resistance should be about  $10^{-10}$  W/K. We find higher conductance than this by a factor as high as five, indicating that electron-phonon interaction may contribute to the cooling of the electron distribution. We anticipate testing nanowires soon with lower  $T_c$ . At lower temperatures we expect reduced electron-phonon thermal contact. We anticipate that similar devices operated with wire temperatures below 1K will be diffusion cooled.

At the ends of the wire the electron state-space changes from one-dimensional to two-dimensional. It is likely that Andreev reflection<sup>14</sup> occurs here, containing the electrons to some degree in the nanowire. We have not yet estimated the size of this effect.



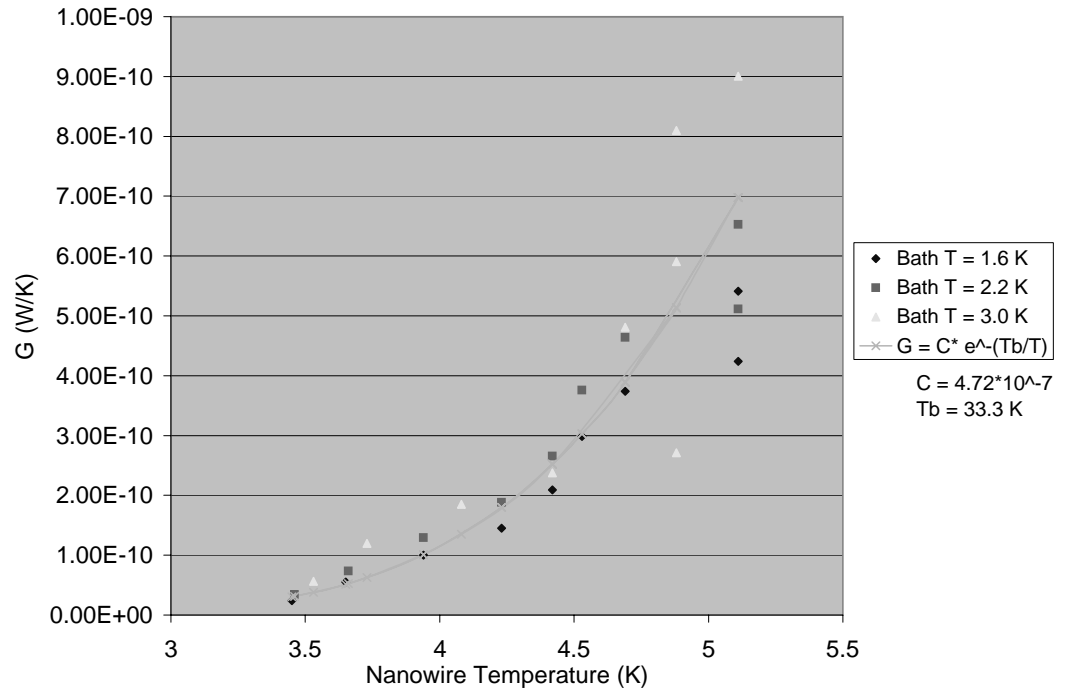


**Figure 4.**

**Thermal Conductance of the Nanowire.** We estimate the effective thermal conductance  $G$  of the nanowire using a simple lumped element thermal model. The values of  $G$  we derive are consistent for all three bath temperatures. The conductance of the wire rises with wire temperature. This is to be expected since the unpaired electron density is a strongly increasing function of temperature near  $T_c$ .



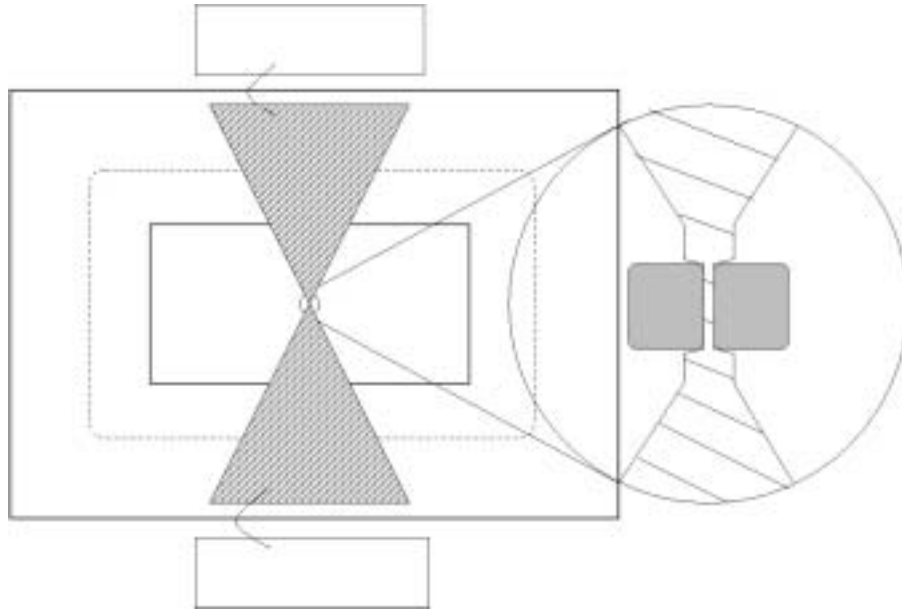


**Figure 5.**

**RF Coupling to Nanowire Bolometer.** The active region of a nanowire bolometer can be created at the apex of a bowtie antenna. A possible layout is drawn here. The bowtie is shown here spanning a rectangular waveguide, the inner perimeter of which is the inner rectangle. The bowtie is lithographed on a thin silicon nitride membrane supported by a thicker silicon frame. The inner edge of the silicon frame is indicated with a dashed line. Bias and output connections can be made with wire bonds to the regions of the bowtie outside the waveguide. The nanowire can be created by milling with a focused ion beam. Areas removed with the beam are shown shaded. By placing the bowtie across a rectangular waveguide the same lithographed device can be used over a wide range of waveguide bands.

## 5. COUPLING RADIATION TO THE NANOWIRE

To use the nanowire as a bolometer it is necessary to connect it to an antenna so that it can act as a load resistor, dissipating the electromagnetic energy from the sky. Terminating an antenna usually requires a resistive impedance in the neighborhood of 50-200 ohms. It should be possible to bias a nanowire at such a dynamic resistance using a low impedance DC bias source (voltage bias). This bias point will be very near the bottom of the return-to-superconductivity portion of the IV curve. At this bias point the IV curve is strongly non-linear which should lead to high responsivity.

A wire which has an impedance near that of free space, and which also has physical dimensions much less than the wavelength of the applied radiation, will act as a simple lumped resistive circuit element. This simplifies the transmission line circuit needed to connect to the wire, and permits very wide absorption bandwidths. The limitation to the bandwidth created by the wire dimensions is about  $10^{16} Hz$ . Because this value is so high, in the UV range, we anticipate that the solid-state physics of radiation absorption that will limit bandwidth, rather than the limitation above, which is derived just from Maxwell's Equations.

In connecting to the nanowire it is necessary to avoid long thin wires to the nanowire since these introduce series inductive reactance. It is also necessary to avoid broad contact regions very close to the nanowire since these create a shunt capacitive admittance. The cleanest way to connect to the wire is to use tapered conductors. There are many ways such a system can be connected to terminate a transmission line from an antenna. One of the simplest may be to taper the center conductor of a suspended microstrip carrying the electromagnetic wave to the nanowire.

For our next round of testing of nanowires we will attempt to create a lithographed wire at the apex of a bowtie antenna which we will place across a rectangular waveguide as shown in figure 5. This proven coupling



structure has the advantage that the same lithographed geometry can be placed across a range of waveguide sizes thereby covering several decades of frequency space. Absorption efficiency exceeding 90% has been achieved across full waveguide bandwidths using this geometry.<sup>15</sup> Also, filters and feed horns in waveguide are available off-the-shelf, allowing us to concentrate on development of the bolometer itself.

## 6. NEXT STEPS

The next step in our study of nanowire bolometers will be to create an AC/DC diplexing circuit and measure  $\sim 10$  MHz responsivity and Noise Equivalent Power of Mo-Ge nanowires. We will also attempt to create lithographed examples using focused ion beam lithography and use these to test the bowtie-in-waveguide coupling structure at millimeter wavelengths. We also intend to test bolometers made with superconducting materials with lower bulk  $T_c$  such as Osmium and Molybdenum.

## 7. ACKNOWLEDGMENTS

We acknowledge helpful discussions with Medhi Asheghi and Rob Schoelkopf. This project was supported by NSF grant OPP 0089140 , NASF Career grant DMR 01-34770, and Sloan grant BR-4148.

## REFERENCES

1. P. L. Richards, "Bolometers for Infrared and Millimeter waves," *J. Appl. Phys.* **76** (1), pp. 1-24, 1994.
2. D. E. Prober, "Superconducting Terahertz mixer using Transition-edge Microbolometer," *Appl. Phys. Lett.* **62** (17), pp. 2119-2121, 1993.
3. M. Nahum and J. M. Martinis, "Ultrasensitive-hot-electron microbolometer," *Appl. Phys. Lett.* **63** (22), pp. 3075-3077, 1993.
4. P. J. Burke, R.J.Schoelkopf, D. E. Prober, A. Skalare, W. R. McGrath, B. Bumble and H. G. LeDue, "Length Scaling of Bandwidth and noise in hot-electron superconducting Mixers," *Appl. Phys. Lett.* **68** (23), pp. 3344-3346, 1996.
5. S. P. Langley, "The Bolometer," *Nature* **24**, pp. 14-16, 1881.
6. N. S. Nishioka, P. L. Richards and D. P. Woody, "Composite bolometers for submillimeter wavelengths," *Appl. Optics* **17** (10), pp. 1562-1567,
7. J. C. Mather, "Bolometer noise: nonequilibrium theory," *Appl. Optics* **21** (6), pp. 1125-1129, 1982.
8. P. L. Richards and Tek-Ming Shen, "Superconductive Devices for Millimeter Wave Detection, Mixing, and Amplification," *IEEE Trans. on Electron Devices* **ED-27** (10), pp.1909-1920, 1980.
9. J. C. Mather, "Bolometers: ultimate sensitivity, optimization, and amplifier coupling," *Appl. Optics* **23** (4), pp. 584-588, 1984.
10. T. Bollinger and A. Bezryadin, to be published.
11. A. Bezryadin, C.N. Lau, and M. Tinkham, "Quantum suppression of superconductivity in ultrathin nanowires," *Nature* **404**, pp. 971-974, 2000.
12. A. D. Zaikin, D. S. Golubev, A. van Otterlo and G. T. Zimanyi, "Quantum phase slips and transport in ultrathin superconducting wire," *Phys. Rev. Lett.* **78**, pp. 1552-1555, 1997.
13. C. Kittel, *Introduction to Solid State Physics*, John Wiley and Sons, Inc, New York, 1956.
14. A. F. Andreev, "The Thermal Conductivity of the Intermediate State in Superconductors," *Soviet Physics JETP* **19** (5), pp. 1228-1231, 1964.
15. D. P. Osterman, R. Patt, R. Hunt and J. B. Peterson, "Antenna-coupled bolometer with a micromachined-beam thermal link," *Appl. Phys. Lett.* **71** (16), pp. 2361-236